Tectonophysics, 165 (1989) 237–250
Elsevier Science Publishers B.V., Amsterdam – Printed in The Netherlands

Seismotectonics and present-day relative plate motions in the Tonga–Lau and Kermadec–Havre region

BERNARD PELLETIER and REMY LOUAT

Office de la Recherche Scientifique et Technique Outre-Mer (ORSTOM), B.P. A5, Nouméa Cedex (New Caledonia)

(Received July 14, 1988; revised version accepted October 28, 1988)

Abstract

Pelletier, B. and Louat, R., 1989. Seismotectonics and present-day relative plate motions in the Tonga–Lau and Kermadec–Havre region. *Tectonophysics*, 165: 237–250.

An updated compilation of shallow seismicity in the Tonga–Kermadec arc and back-arc region, including especially 304 focal mechanisms from centroid moment tensor solutions files, provides new insights on the present-day tectonics and allows the relative motions between the Pacific, Indo-Australian and Tonga–Kermadec plates to be quantified.

Azimuths of slip vectors along the trench change at 19°S. In the southern domain (35–19°S) the mean azimuth ranges from N280°E to N285°E, while in the northern domain it trends N276–277°E. This 19°S boundary also exits in the back-arc domain. South of 19°S, from 35°S to 20°S the direction of back-arc extension is respectively N135°E, N122°E and N111°E within the southern Havre trough, northern Havre trough and southern Lau basin. In the southern Lau basin the N111°E opening direction is compatible with the trend of the newly mapped Valu Fa ridge. North of 19°S, in the northern Lau basin (16–18°S), a N93°E trending crustal extension occurs along the N135°E Peggy ridge and along an inferred N5–10°E spreading zone. Between these two extensional features a fourth plate, the northern Lau microplate, is present. At 18–19°S a ridge–ridge–ridge triple junction, accommodated by N95°–115°E right-lateral strike-slip fracture zones, is proposed at the complex transitional zone between the southern and the northern parts of the Lau basin. The Fiji–North Tonga fracture zone which bounds northward the Lau back-arc basin is composed of two segments: a N95°E eastern segment extending from the northern end of the Tonga trench to 178°30′W, and a N75°E western segment lying north of the Fiji platform. A ridge–fracture–fracture triple junction is inferred at 178°30′W–15°45′S between the northern end of the Peggy ridge and the two segments of the Fiji–North Tonga fracture zone.

Using the model RM-2 of Minster and Jordan (1978) and the directions of back-arc spreading and convergence at the trench, relative plate motions are estimated. The extension rates in the back-arc domain increase northward, and are respectively 0.8, 2.1 and 8 cm/y at 33°S, 28°S and 24°S. Farther north parallelism between directions of different motions does not allow the calculation of any accurate result. Therefore north of 24°S we used a spreading rate of 8 cm/y which corresponds to the 24°S result and also to the value deduced from magnetic anomalies. The consumption rates along the Tonga–Kermadec trench are respectively 7.2, 9.6, 16.4, 17.1 and 17.8 cm/y at 33°S, 28°S, 24°S, 20°S and 17°S. Both the back-arc opening rate and the consumption rate of the Pacific plate sharply increase between the northern Havre trough and the southern Lau basin. This limit coincides with the Louisville ridge–trench junction. Along the N95°E eastern segment of the Fiji–North Tonga fracture zone, a pure left-lateral strike-slip motion, parallel to the N93°E opening tectonics within the northern Lau basin occurs. In contrast along the N75°E western segment of the Fiji–North Tonga fracture zone, a left-lateral strike-slip motion of 7 cm/y should be accompanied by a N135°E extensional motion of 3.5 cm/y.

Introduction

Reconstruction of the history and the determination of the sense of extensional motion in back-arc basins present difficulties, because these marginal basins are generally small and located near unstable plate boundaries. Moreover, their structural and magnetic patterns are complex and

0040-1951/89/$03.50

the magnetic anomalies are often difficult to identify. Consequently these areas are subject to different interpretations and speculations. This is also the case for the Tonga–Kermadec arc and Lau–Havre region in the Southwest Pacific, which corresponds to a segment of the Pacific–Indo-Australian plate boundary and where crustal extension behind the arc and convergence at the trench occur simultaneously. Using bathymetry, sediment distribution, heat flow and geology of neighbouring islands, Karig (1970) firstly suggested that the active Lau–Havre basin, elongated N–S and located between the active Tonga–Kermadec arc and the Lau–Colville remnant arc, resulted from crustal extension since the late Miocene. Following this idea and on the basis of new geological (petrography) and geophysical (mainly marine magnetic anomalies) data, numerous models concerning the tectonic history of the Lau basin have been proposed (Chase, 1971; Sclater et al., 1972; Hawkins, 1974; Gill, 1976; Lawver et al., 1976; Weissel, 1977; Cherkis, 1980; Malahoff et al., 1982; Larue et al., 1982; Ruellan et al., 1989). However, the age of the onset of spreading, the location of multiple spreading centers and transform faults, and the sense of extensional motion largely differ in these models, the same topographic features being interpreted either as a spreading center or transform fault.

Assuming that shallow seismicity reflects the stress state in the crust and is closely associated with the structural pattern, the distribution of shallow earthquakes and their focal mechanism solutions are valuable in characterizing the present-day tectonics in the active trench and back-arc regions. Previous seismicity studies of the Tonga–Kermadec region were mainly focused on the Wadati-Benioff seismic zone and the Pacific plunging plate (Isacks et al., 1969; Sykes et al., 1969; Johnson and Molnar, 1972; Chen and Forsyth, 1978; Billington, 1980; Louat and Dupont, 1982). However, these authors also described several discrete zones of inter-arc shallow earthquakes lying outside the main Tonga–Kermadec seismic zone, especially within the Lau basin and between Fiji and the northern end of the Tonga trench. The different tectonic interpretations of Chase (1971) and Sclater et al. (1972) used the shallow seismicity distribution to infer active boundaries between different microplates. The latest seismotectonic study of the back-arc region was published by Eguchi (1984) who described only the shallow seismicity in the northernmost Lau basin and added eleven new focal mechanism solutions to the single solution of Isacks et al. (1969). Eguchi (1984) proposed: (1) a left-lateral shear zone between Fiji and the northern Tonga trench; (2) a NW–SE opening tectonics in the northern Lau basin.

Since the study of Eguchi (1984) a large amount of new data is available owing to the world seismological network. This paper presents an updated compilation of shallow seismicity and focal mechanism solutions data from the Tonga–Kermadec trench and the Lau–Havre back-arc basin. The main objective is to characterize the present-day tectonics and the sense of plate motions, and to provide new constraints for the tectonic reconstructions.

Data set

Figure 1 shows shallow foci (depth 0–70 km) located by 50 or more seismological stations and obtained from the International Seismological Centre (ISC) catalogue for the period 1964–1982, and from Preliminary Determination of Epicenters (PDE) monthly bulletins for the period 1983–November 1987. For the period 1985–November 1987 only earthquakes with a focal mechanism solution have been considered.

Focal mechanism solutions used in this study are issued from two data sets. The first set (FMPS) is obtained from literature (Isacks et al., 1969; Johnson and Molnar, 1972; Chen and Forsyth, 1978; Billington, 1980; Everingham, 1983; Eguchi, 1984). Most FMPS mechanisms are first motion fault plane solutions. The second data set (CMTS) is constituted by 304 moment tensor solutions for the January 1977–November 1987 period. Events until March 1984 are obtained with the centroid moment tensor method (Dziewonski and Woodhouse, 1983; Dziewonski et al., 1983a, b, c; 1984a, b, c; Giardini, 1984; Giardini et al., 1985) and events since April 1984 are centroid moment tensor solutions given by PDE monthly bulletins.

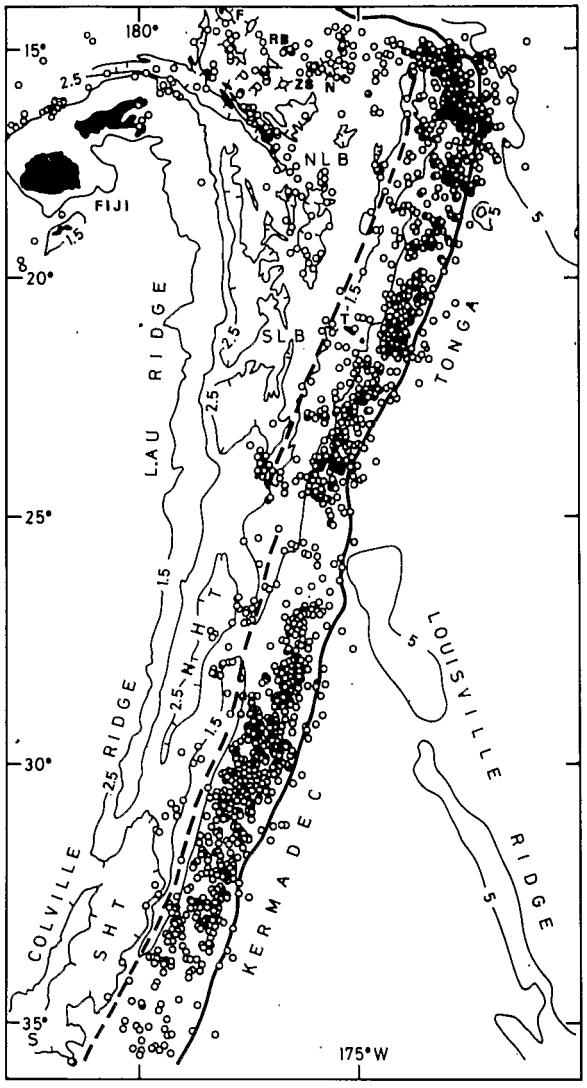

Fig. 1. Shallow-seismicity map (0–70 km depth) in the Tonga–Kermadec/Lau–Havre region. Earthquakes are from ISC catalogue (1964–1982), PDE bulletins (1983–November 1987). For the period 1985–November 1987 only events given by CMTS files are used. Bathymetry map is from Kroenke et al. (1983); depths are in kilometers. Heavy and heavy-dashed lines represent respectively the Tonga–Kermadec trench axis and the active Tonga–Kermadec volcanic arc. SHT—southern Havre trough, NHT—northern Havre trough, SLB—southern Lau basin, NLB—northern Lau basin, PR—Peggy ridge, T—Tongatapu island, N—Niuafo'ou island; ZS—Zephir shoal, RB—Rochambeau bank, F—Futuna island.

Only 20 among 53 FMPS solutions have been considered (Fig. 4). The FMPS mechanisms related with the underthrusting motion of the Pacific plate have not been used because a large number of CMTS focal mechanisms is available. In contrast, FMPS events located in the back-arc area (fifteen events) and in the vicinity of the trench (five events) have been used in order to have available the greatest amount of data. Computation of plate motions only takes account of the CMTS data set because this latter is more coherent than the FMPS one.

Shallow-seismicity distribution and focal mechanisms

The distribution of shallow earthquakes plotted on Fig. 1 delineates three seismic domains, as previously mentioned by Sykes (1966), Isacks et al. (1969) and Sykes et al. (1969): a high density seismic zone between the Tonga–Kermadec arc and trench, a diffuse seismic zone along the Lau–Havre back-arc basin and an E–W trending seismic belt from the Fiji islands to the northern end of the Tonga trench.

The main Tonga–Kermadec seismic zone

The highly active seismic zone striking N20°E is related to the descending of the Pacific plate below the Tonga–Kermadec arc. Most events occur between the trench axis and the volcanic line. Additional seismic activity is also located at the trench and east of it; these events are associated with the bending of the Pacific plate (Chen and Forsyth, 1978). In detail, the seismicity distribution shows large-scale irregularities along the arc.

A 200 km long gap exists where the Louisville ridge, a major topographic feature supported by the Pacific plate, intercepts the trench at 26°S. Because this gap is not in the direct prolongation of the ridge but perpendicular to the trench in front of the junction point, the buoyancy of the ridge proposed by Kelleher and McCann (1976) seems unlikely to play a major role in the existence of the gap (Louat and Dupont, 1982). This gap results probably from creeping within a thick active contact zone where the ridge subducts, provoking an erosion of the lower slope of the arc by underthrusting (Pelletier, 1989).

A relatively quiet seismic zone also exists south of 33°S. Up to now this zone cannot be sufficiently explained. However, we note here a gentle

southward shallowing of the trench accompanied by a narrowing and deepening of the arc.

The northernmost part of the Tonga trench is characterized by far greater seismic activity than elsewhere in the arc. This area corresponds to the westward curvature of the trench. At this place, the events located east of the trench are particularly numerous.

The slip vector azimuth from interplate thrust-type focal mechanism solutions gives the relative motion between the Pacific plate and the Tonga–Kermadec arc. Trends of nodal plane poles chosen as the direction of the slip vector of 168 interplate thrust-type solutions are shown on Fig. 2, and plotted against latitudes of the epicenters on Fig. 3. Most azimuths range from 260° E to 300° E. On each side of the Louisville Ridge gap the mean azimuth of the slip vectors is almost equivalent. Matching our data with the calculated slip vector azimuths between the Pacific and Indo-Australian plates from the model RM-2 of Minster and Jordan (1978), two domains separated by a break at 19° S can be identified (Fig. 3). South of 19° S (domain A) the mean azimuth is above the RM-2 value. In contrast, north of 19° S the N276° E mean azimuth of the B domain is slightly below the N277.5–278° E RM-2 value. Within domain A, the mean azimuth increases from south to north. A least-square regression calculated for the domain A gives a positive slope of 0.4° for each degree of latitude from N278.2° E at 36° S to N285.6° E at 19° S. The discrepancy between the mean slip vector azimuths and the values from the model RM-2 slightly increases northward.

Along the main Tonga–Kermadec seismic zone, 79 solutions (CMTS) differ from interplate thrust-type solutions (Fig. 4). Most of these mechanisms document normal faulting near the trench. Active normal faults are always parallel to the trench axis, even near the Louisville ridge area where the trench is shifted and strikes N–S and in the northernmost area where the trench bends sharply westward. Four events with normal fault solutions cluster at the Louisville ridge–trench intersection area. In addition to the set of normal fault solutions, two clusters of foci associated with thrust focal mechanism solutions are present east

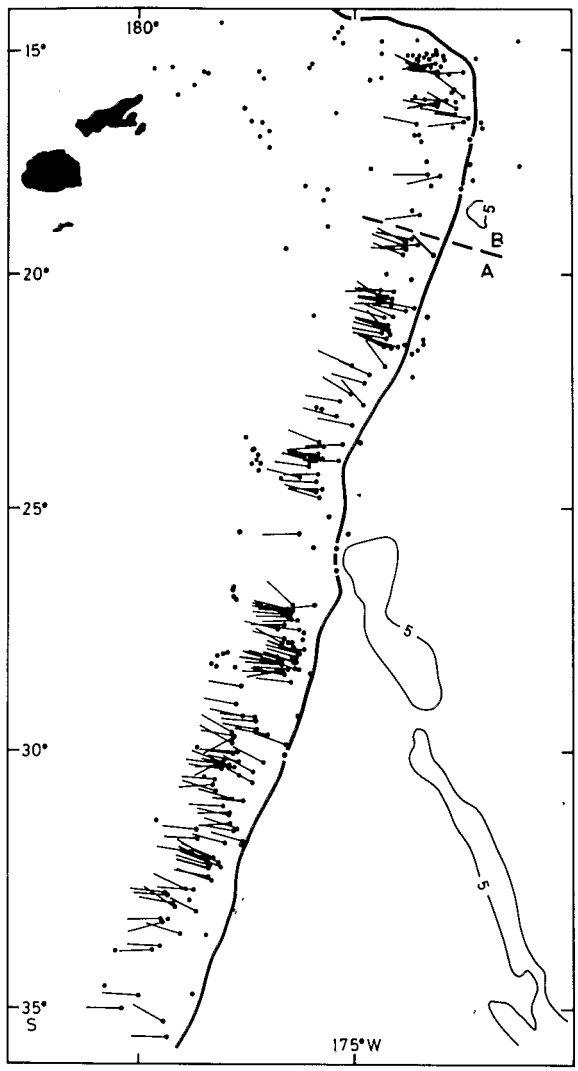

Fig. 2. Slip vectors along the Pacific–Tonga Kermadec plate boundary. Dots indicate locations of the 304 earthquakes from CMTS file (1977–November 1987). Sense of seismic slip motion is reported for 168 inter-plate thrust focal mechanism solutions. Heavy line represents the Tonga–Kermadec trench axis. Heavy dashed line at 19° S delineates the boundary between the southern A and northern B domains.

of the trench (Fig. 4). The first group, six CMTS events centered at 21° 30′ S and aligned along a N20° E trend, has a *P*-axis perpendicular to the trench; these solutions are likely connected to the bending of the plate. The second group located around 17° S is aligned along a N135° E direction and has a *P*-axis ranging from ENE–WSW to NE–SW. These solutions could be associated with the complex pattern characterizing the northern

closure of the Tonga trench where tearing of the Pacific plate occurs (Isacks et al., 1969; Louat and Dupont, 1982). In spite of the complexity of the northern area which includes thrust, normal fault and strike-slip motions, three observations can be put forward (Fig. 4): (1) the *T*-axis turns progressively with the trench from E–W to N–S; (2) from southeast to northwest focal mechanisms document thrust faulting with a NE–SW *P*-axis, strike-slip faulting with a NE–SW *T*-axis, normal faulting with a NE–SW *T*-axis, and finally normal faulting with a N–S *T*-axis and vertical faulting with the northern compartment uplifted; (3) epicenters of earthquakes showing a strike-slip motion are aligned along a N–S direction and events showing E–W normal faulting and vertical faulting are distributed along an E–W strike. These data suggest a progressive evolution from normal subduction to a tearing of the Pacific plate via a differential N–S stretching accommodated by N–S trending left-lateral strike-slip motion. In our interpretation most of the seismic activity occurs within the underthrusting plate. However, a cluster of events with normal fault solutions (five events with an averaged NE–SW *T*-axis) is located just east of the volcanic line within the overthrusting plate. We explain these peculiar extensional tectonics in the arc as the result of first the tearing and then sinking of the lower plate (Louat and Dupont, 1982).

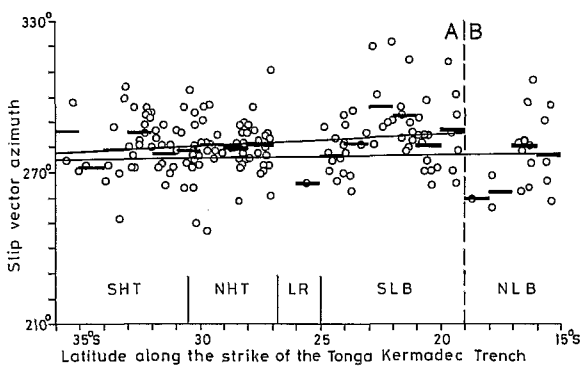

Fig. 3. Azimuths of slip vectors from thrust-type solutions along the Pacific–Tonga Kermadec plates boundary. Heavy segments represent the average slip vector azimuth for each degree of latitude. A similar result is obtained by weighting each slip direction with the seismic moment of the corresponding earthquake. The lower continuous line indicates the relative motion between Pacific and Indo-Australian plates, calculated from the model RM-2 of Minster and Jordan (1978), assuming no back-arc spreading. Vertical dashed line marks the 19°S boundary between the domains A and B shown in Fig. 2. In domain A, the upper line is the least-square regression. Locations of the Louisville ridge (LR)–trench intersection and the different back-arc domains (SHT—southern Havre trough, NHT—northern Havre trough, SLB—southern Lau basin, NLB—northern Lau basin) are also shown.

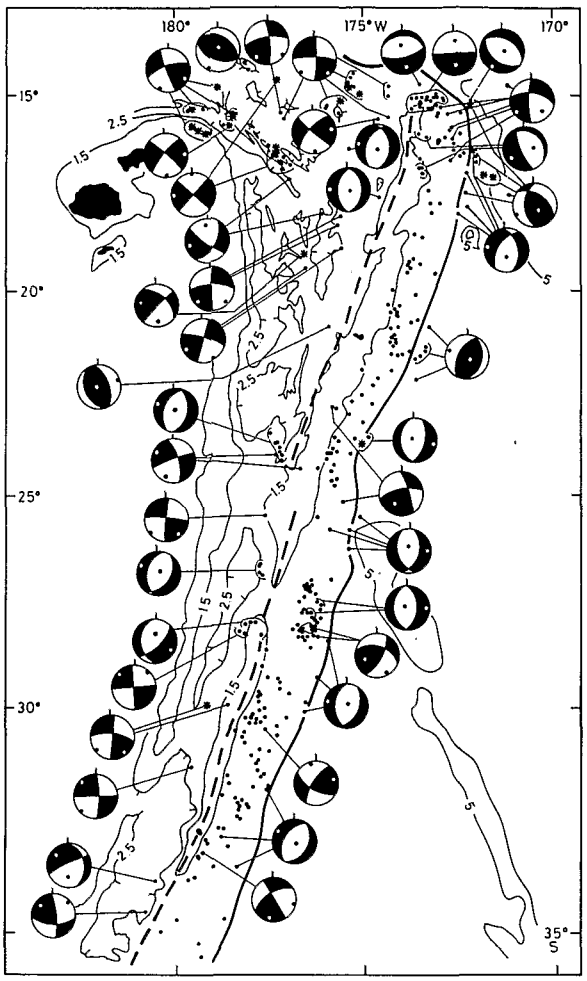

Fig. 4. Compilation of focal mechanisms for shallow earthquakes (0–70 km) in the Tonga–Kermadec/Lau–Havre region excluding the thrust solutions characterizing the Pacific–Tonga Kermadec plate contact presented in Fig. 2. Dots are locations of CMTS events. Stars indicate previously published solutions. A cluster of earthquakes showing similar solutions is illustrated by a single focal mechanism.

The Havre–Lau back-arc basin

The back-arc domain lying between the Tonga–Kermadec arc and the Lau–Colville ridge

is "Y"-shaped, its width ranging from 120 km in the south to 450 km in the north. In detail, the back-arc domain consists of several troughs. From south to north, they are the southern Havre trough (SHT) reaching more than 4000 m depth, the northern Havre trough (NHT), and the Lau basin (Fig. 1). The latter is the largest and has an average water depth ranging from 2000 to 2500 m. Its detailed morphology is complex and up to now poorly mapped. The Lau basin can be divided into two parts by using the seismic data: the southern Lau basin (SLB) between 24–25°S and 19–20°S, and the northern Lau basin (NLB) between 16° and 19°S. The NW–SE trending Peggy ridge (PR) is the major topographic feature of the NLB.

In contrast to the main Tonga–Kermadec seismic zone, the seismicity of the back-arc domain is scattered (Fig. 1). However, it delineates discrete zones. The number of earthquakes diminishes southward from the Lau to the Havre troughs. In the south, the events are restricted along the eastern side of the Havre troughs.

In the Lau basin four seismic zones can be differentiated (Fig. 1). (1) A continuous NW–SE linear belt of earthquakes between 16° and 18°S coincides with the Peggy ridge. (2) A 100 km wide N–S zone lies in the center of the Lau basin between 18° and 20°S; it is in the southern prolongation of the Peggy ridge and fits with the deepest depression elongated N–S. (3) A third seismic area coincides with the southern limit of the SLB; this cluster occurs at the same latitude as the shift of the trench axis. (4) The fourth seismic area is located in the northeastern part of the Lau basin where epicenters are scattered around small-scale depressions.

Compilation of focal mechanism solutions within the Havre–Lau back-arc basin is represented in Fig. 4. From 35° to 23°S, all focal mechanism solutions (24 CMTS and 1 FMPS from Johnson and Molnar, 1972) are normal fault and strike-slip fault with a coherent direction of *T*-axis. Three observations have to be made for this area: (1) normal fault type solutions predominate at the latitude of the troughs while strike-slip type solutions are seen at the saddles; (2) from south to north, the *T*-axis turns slightly from SE–NW to ESE–WNW; the averaged *T*-axis directions are, respectively for SHT, NHT and SLB, N135°E, N122°E and N111°E; (3) *T*-axes from strike-slip type solutions in the saddles are closer to a N–S direction than those from normal fault solutions.

Along the Peggy ridge, the six CMTS solutions shown on Fig. 4 are consistent with the three FMPS previously published solutions by Billington (1980) and Eguchi (1984). All focal mechanisms are strike-slip type solutions sharing a common E–W *T*-axis. The two southernmost solutions along the Peggy ridge show an E–W extensional component. Because two events (1 CMTS, 1 FMPS) located around 15°50′S, 178°40′W have the same solutions as events characterizing the middle part of the ridge, we propose that the fault associated with the Peggy ridge extends up to 16°S. Focal solutions and the linear trend of seismicity suggest a NW–SE trending strike-slip motion along the Peggy ridge as proposed by Eguchi (1984). The northern Lau basin east of the Peggy ridge is characterized by two clear normal fault type solutions with a sub-E–W *T*-axis. At 15°45′S, 174°45′W, an event with strike-slip type solution showing also an E–W *T*-axis is present. The mean *T*-axis direction of all the ten CMTS solutions (including strike-slip and normal faults) between 16° and 18°S is N93°E (see Figs. 6 and 7).

In the central part of the Lau basin just south of the Peggy ridge, all solutions (4 CMTS and 1 FMPS) are strike-slip. They can be classified in four groups (Fig. 4): (1) the northwesternmost event (18°10′S, 176°10′W) shows a normal faulting component and is similar to the southernmost event of the Peggy ridge; (2) two solutions (18°20′S, 175°40′W) have a NE–SW (N53°E) *T*-axis; (3) a FMPS solution (19°S, 176°30′W; Eguchi, 1984) has a N97°E *T*-axis; and (4) the two latest solutions (in the south) have a N70°E *T*-axis. We note also an unexpected thrust-type solution at 21°S along the eastern edge of the Lau basin (Fig. 4).

In summary, the focal mechanism solutions suggest that two domains exist in the back-arc basin: a southern one including SHT, NHT and SLB with a SE–NW to ESE–WNW extension, and a northern one (NLB) with a sub-E–W extension. These two domains are separated by a com-

plex transitional zone around 19–20°S showing strike-slip type solutions with NE–SW to ENE–WSW *T*-axes.

The Fiji–North Tonga fracture zone (FNTFZ)

A sub-E–W seismic belt extends at the northernmost part of the Lau basin along 15°S from the western edge of the Tonga arc to Fiji islands (Fig. 1). In detail, it comprises two distinct seismic segments. The eastern one of 120 km wide trends N95°E from 173°30′W to 178°30′W, and is superimposed on a poorly known area including discontinuous topographic highs (Niuafo'ou island, Zephir shoal, Rochambeau bank). Its northern limit just passes south of the Futuna island. The western segment stretches from 178°20′W to the north of the Fiji islands along a N75°E trend. The seismicity delineates a 40–50 km wide belt and is mainly confined along a linear tight depression located north of the Fiji platform. The variation in trend as well as in width between these two seismic segments occurs at 178°30′S just southwest of the Futuna island where the Peggy ridge intercepts the FNTFZ (Fig. 1).

With an exception of two events, the focal solutions all along the FNTFZ suggest an E–W trending left-lateral strike-slip motion as proposed by Isacks et al. (1969) and Eguchi (1984). However, each segment previously described is different in detail. Eleven events (5 CMTS + 3 FMPS) occurring in the western segment suggest a N255°E left-lateral strike-slip motion (Figs. 4 to 7). In the eastern segment, 13 (10 CMTS + 3 FMPS) similar mechanisms document a N275°E left-lateral strike-slip motion. Two additional solutions are noted: a thrust-type just south of Futuna with a NE–SW *P*-axis consistent with the one of the thirteen previously mentioned strike-slip solutions; and a strike-slip solution with a SE–NW

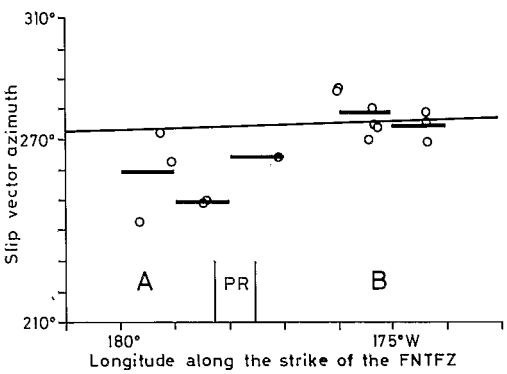

Fig. 5. Slip vector azimuths along the Fiji–North Tonga fracture zone (FNTFZ). Only CMTS solutions suggesting a left-lateral strike-slip motion have been used (15 among 17). The northern end of the Peggy ridge (PR) and the western (A) and eastern (B) segments of the FNTFZ are shown. The lower continuous line indicates the relative motion between Pacific and Indo-Australian plates calculated from the model RM-2 of Minster and Jordan (1978).

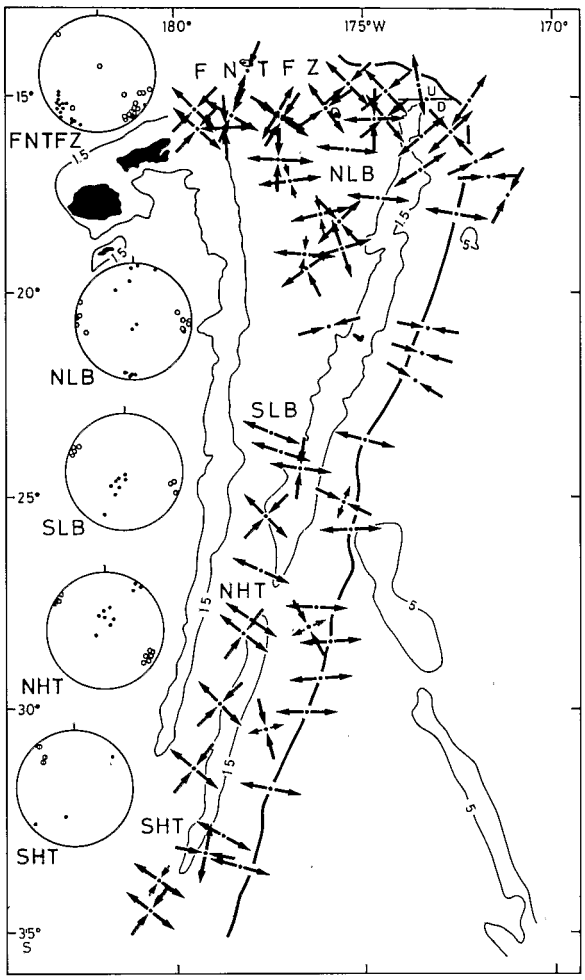

Fig. 6. Map showing the direction of sub-horizontal principal stress axes for the Tonga–Kermadec/Lau–Havre region. Convergent arrows indicate *P*-axis from thrust solutions, divergent arrows indicate *T*-axis from normal fault solutions. Both *P* and *T*-axes are drawn for strike-slip solutions. Insets show stress axes for the fourth back-arc areas and for the Fiji–North Tonga fracture zone (FNTFZ). *P*-axes are indicated by filled circles and *T*-axes by open circles.

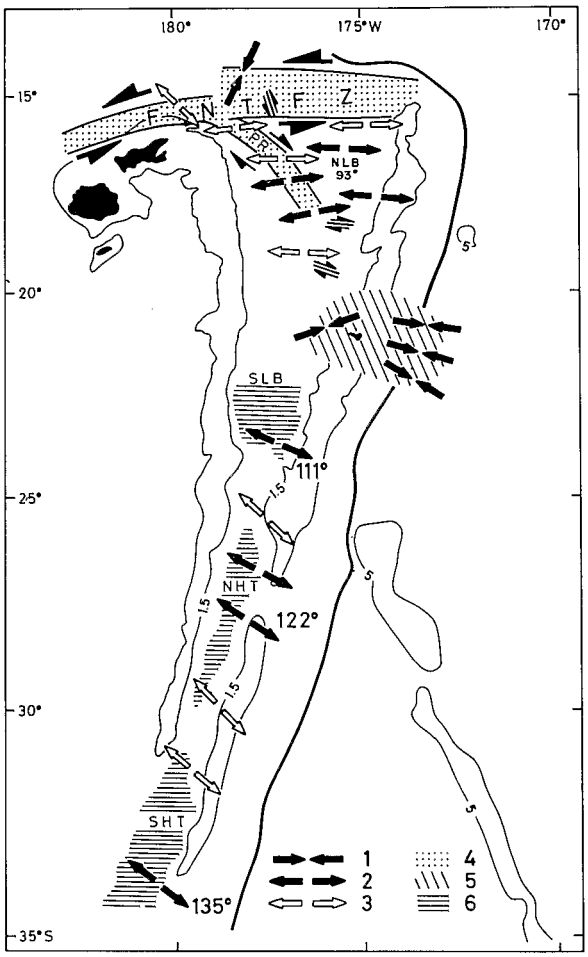

Fig. 7. Inferred seismotectonics of the Havre–Lau back arc basin. *1* = *P*-axis given by thrust solutions, *2* = *T*-axis given by normal fault solutions, *3* = *T*-axis given by strike-slip solutions. Filled and opened divergent arrows show direction of opening; for each back-arc area, a mean direction of *T*-axis is given (93°, 111°, etc...). *4* = tectonic features defined by seismic linear belt, *5* = domain with unexpected thrust solutions, *6* = back-arc troughs south of 22°S.

P-axis which is difficult to interpret because it is reverse in relation to the others. This solution documents possibly a N–S trending left-lateral strike-slip motion. On each side of 178°30′W, the average slip vectors are parallel to the strikes of the seismic segments. Azimuths of slip vector from left-lateral strike-slip solutions are plotted along the strike of the FNTFZ and are compared (Fig. 5) with the slip motion calculated from the model RM-2 of Minster and Jordan (1978). Along the eastern segment (B) observed slip vectors fit with the calculated RM-2 ones. In contrast, slip vectors azimuths are 20° below the RM-2 values along the western segment (A).

Discussion and relative plate motions

There exist three major plates in the area: the Pacifc plate (P), the Indo-Australian plate (IA) and the small Tonga–Kermadec plate (TK). In the northern part of the studied area, a supplementary North-Lau microplate exists (NL). To compute the relative motions, the NL microplate will be arbitrarily attached to the TK plate. Using the model RM-2 of Minster and Jordan (1978), our data allow the motions TK–P, IA–TK and IA–P to be estimated.

Subduction and back-arc spreading along the Tonga–Kermadec arc

South of 19°S azimuths of slip vectors from interplate thrust related to the Pacific plunging plate are higher than those predicted by the model RM-2. In contrast, north of 19°S they are slightly lower (Fig. 3). Assuming that the discrepancy is only due to back-arc opening, the direction of the back-arc extension has to change around 19°S and has to be in the N97°–187°E window in the southern domain (A) and in the N7°–97°E window in the northern domain (B). Focal mechanism data in the back-arc domain are in good agreement with these inferred directions of extensional motion. Indeed, we find: (1) a SE–NW to ESE–WNW extensional tectonics in the southern back-arc domain (N135°, 122° and 111°E respectively for SHT, NHT and SLB areas); (2) an E–W extensional tectonics in the northern Lau basin (N93°E in NLB); (3) a transitional zone with complex solutions near 19°S.

The direction of motion IA–TK given by the back-arc opening trend (Figs. 6 and 7), the direction of motion TK–P given by the azimuth of the slip vectors at trench (Figs. 2 and 3) and the motion IA–P given by the model RM-2 of Minster and Jordan (1978) enable the complete vector diagram to be constructed. The vector diagram is calculated at the SHT, NHT, SLB and NLB latitudes because each back-arc basin has its own direction of extension (Table 1, Fig. 8). In the northern part of the SLB and in the NLB, di-

TABLE 1

Relative plate motions in the Tonga–Kermadec area deduced from this study.

Latitude, °S	Motion TK–P Slip vector		Motion IA–TK Back-arc extension		Motion IA–P Model RM-2	
	direction (°E)	velocity (cm/y)	direction (°E)	velocity (cm/y)	direction (°E)	velocity (cm/y)
33	279.53	7.2 ± 0.2	135	0.8 ± 0.2	275.6	6.6
28	281.85	9.6 ± 0.5	122	2.1 ± 0.5	276.3	7.6
24	283.7	16.4 ± 2	111	8 ±2	276.8	8.5
20	285.55	23 ±5	111	14 ±5	277.3	9.2
20 *	283.65	17.1	111	8	277.3	9.2
17	276.71	–	93	–	277.7	9.8
17 *	275.57	17.8	93	8	277.7	9.8

* Computation with a 8 cm/y back-arc spreading rate deduced from magnetic anomalies in the Lau basin. Uncertainty on the velocities is calculated with 1° of deviation on the azimuth of slip vector at trench or the direction of extension.

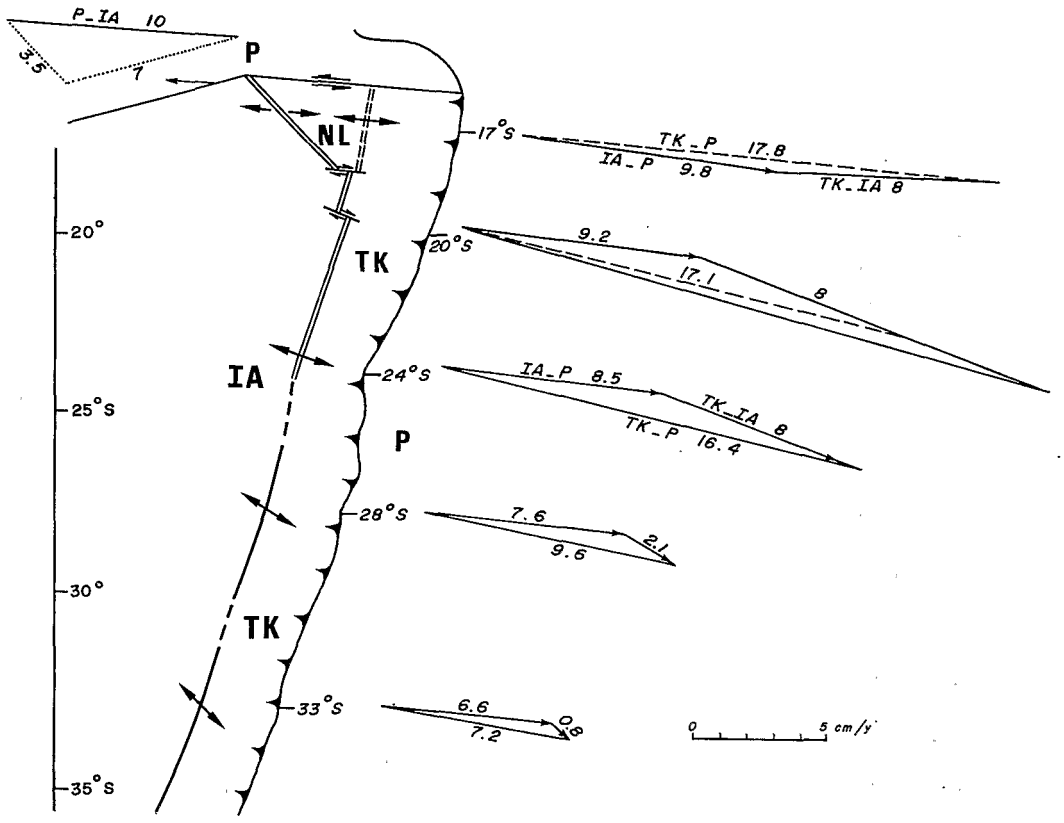

Fig. 8. Inferred plate boundaries and relative motions in the Tonga–Kermadec region. P—Pacific plate; IA—Indo-Australian plate; TK—Tonga-Kermadec plate; NL—North Lau microplate. For computation P is assumed fixed and NL is attached to TK. Vector diagrams are constructed at 33, 28, 24, 20 and 17°S. Numbers around triangles indicate velocities in cm/y. For 20° and 17°S dashed lines correspond to the motion TK–P using a 8 cm/y back-arc spreading rate. Motion P–IA along the western segment of the Fiji–North Tonga fracture zone is split into two components shown by dotted lines. Divergent arrows indicate directions of back-arc extension. Single line and discontinuous line indicate respectively extension center in troughs and saddles of the Havre domain; double line and discontinuous double line indicate spreading centers and inferred spreading center in the Lau basin; barbed line marks the Tonga–Kermadec trench.

agrams cannot be constructed with our data alone because the angular difference between slip vector at the trench and the direction of back-arc extension is too small to give an accurate value. Indeed a small variation in the direction of extension or in the slip vector azimuth changes drastically the back-arc spreading and consumption rates. In the south, larger angular differences induce small errors and allow accurate values to be calculated (see Table 1). For the NLB and the northern part of the SLB we used a back-arc spreading rate of 8 cm/y deduced from magnetic anomalies and from our result at 24°S. Figure 8 clearly shows that the back-arc extension rate increases from south to north (from 0.8 to 8 cm/y) and jumps at the latitude 25°S from 2.1 to 8 cm/y. Similarly consumption rate along the Tonga–Kermadec trench increases from 7.2 to 17.8 cm/y and jumps from 9.6 to 16.4 cm/y at 25°S. This sudden increase in velocities corresponds to the transition between the Lau and Havre basins, which coincides with the arrival at the trench of the Louisville ridge.

In the SHT and NHT, the direction of extension proposed here (N135°E and N122°E) agrees well with the N30°E magnetic anomalies lineations described by Malahoff et al. (1982). However, these authors proposed a 5.4 cm/y full spreading rate, which is much larger than our estimate (0.8–2.1. cm/y). We must note here that seismic activity within the Havre back-arc area is only confined along the eastern edge of the basin. This observation could suggest that although it is clear that active extensional tectonics occurs, active spreading may not yet exist.

In the SLB (at 24°S) the 8 cm/y opening rate inferred here is in the same range as the various full spreading rates deduced from studies of magnetic anomalies (7.6 cm/y: Weissel, 1977; 5–5.5 cm/y: Cherkis, 1980; 7 cm/y: Larue et al., 1982; 7.4 cm/y: Foucher et al., 1986). We find a present-day ESE–WNW opening at 24°S (N111°E). The slip vector azimuths at the trench require a similar opening direction between 19°S and 24°S. Several directions of spreading have been proposed for the Lau basin. Previous authors studying seismicity distribution and seismic slip motion have suggested a N135°E opening parallel to the Peggy ridge, which was consequently considered as a transform fault (model C of Sclater et al., 1972; Eguchi, 1984). Although the pattern of magnetic lineation is unclear in detail (Lawver et al., 1976), there is an agreement to conclude that magnetic lineations strike N–S in the central part of the Lau basin from 17° to 21°S (Weissel, 1977; Cherkis, 1980; Larue et al., 1982; Ruellan et al., 1989). From 22° to 24°S, Larue et al. (1982) proposed NE–SW trending lineations. Using magnetic lineations, Weissel (1977) and Cherkis (1980) postulated an E–W opening. Recent new detailed investigations within the Lau basin have shown: (1) a linear ridge named the Valu Fa ridge (Morton and Sleep, 1985), located 40 km west of the active volcanic line (the Tofua arc) and trending N15–20°E over more than 200 km, from 20°50′S to 22°40′S (Foucher et al., 1988; Ruellan et al., 1989); (2) a NNE–SSW active spreading segment over 50 km in the central part of the basin near 18°40′S (Von Stackelberg et al., 1985); (3) a set of N45°E trending strike-slip faults near 20°S and 22°S which offset a N–S oceanic structural grain (Ruellan et al., 1989). The Valu Fa ridge firstly interpreted as an active back-arc spreading center (Morton and Sleep, 1985) has also been considered as a volcanic line resulting from migration of the volcanic front of the arc system to the back-arc domain (Foucher et al., 1988). The N45°E structural lineation has been interpreted as a flow line indicating a NE–SW direction of opening along a N–S spreading center located in the central part of the Lau basin (Ruellan et al., 1989). Among all the different tectonic elements mapped in the SLB, the N15°E Valu Fa structure and the NNE–SSW spreading segment at 18°40′S are compatible with the extensional direction deduced from the CMTS data exposed in this paper. If we assume an oblique N45°E crustal extension along a N–S spreading center as proposed by Ruellan et al. (1989), another plate boundary should exist in the SLB to give an ESE–WNW relative motion TK–P compatible with the observed slip vectors. This boundary could be the Valu Fa ridge as suggested by Ruellan et al. (1989), along which they proposed an extension accompanied by a right-lateral strike-slip motion. However according to this model, a vectorial analysis would imply that the N15°E right-lateral strike-slip motion speed would

have to be about 14 cm/y and more or less equivalent to the N45°E spreading rate. This interpretation seems unlikely, because it is not supported by any seismological data (lack of seismicity along Valu Fa ridge, for example). Taking account of all the available data and especially the seismic ones, we favor a more simple model, that is to say a ESE–WNW (N111°E) opening tectonics in the SLB, which may be located along the Valu Fa ridge. This present-day direction of extension is considered to be very recent. Previous stages of the tectonic development of the Lau basin certainly require another direction of extension.

In the NLB (15°S to 18°S) seismotectonics data infer a present-day sub-E–W resultant motion between the northern parts of the Lau ridge and the Tonga arc. This area includes the Peggy ridge which was interpreted either as a N135°E spreading center (Chase, 1971; models A and B of Sclater et al., 1972) or as a right-lateral transform fault (model C of Sclater et al., 1972; Weissel, 1977; Eguchi, 1984). According to Weissel (1977), the Peggy ridge cuts magnetic anomaly 2′ and is thus a relatively recent tectonic feature. Focal mechanism solutions and seismicity along the Peggy ridge suggest a right-lateral strike-slip motion as earlier proposed by Eguchi (1984). However, if the Peggy ridge acts as a pure right-lateral strike-slip fault, this implies a N–S extensional motion in the northernmost part of the Lau basin along the eastern segment of the Fiji–North Tonga fracture zone (FNTFZ). Opening tectonics more or less parallel to the N95°E eastern seismic segment of the FNTFZ is required along the Peggy ridge, because (1) no solution with N–S *T*-axis is known in the northernmost Lau Basin and (2) the slip vectors from strike-slip solutions along the FNTFZ fit well with the RM-2 ones (Fig. 5) and are parallel to the FNTFZ trend. The mean N93°E direction of the *T*-axis from CMTS solutions compiled within the NLB largely supports this interpretation. In this model, the right-lateral strike-slip component along the Peggy ridge (55% of motion) is almost equal the NE–SW extensional component (45% of motion), the resultant being a sub E–W extension (Fig. 8).

East of the Peggy ridge, two clear normal fault solutions suggest the presence of an unmapped extensional feature (Figs. 7 and 8). These data favor the existence of a fourth plate, the northern Lau microplate (NL) as suggested by Chase (1971), lying between the Peggy ridge, the FNTFZ and this inferred spreading center. The latter would strike N5°–10°E, more or less parallel to the Valu Fa ridge and could form the northern prolongation of it (Fig. 8).

The transitional zone between the SLB and NLB around 18–19°S is characterized by a cluster of shallow earthquakes and by six strike-slip focal mechanism solutions. This area appears complex and difficult to interpret. If we focus on the sub-horizontal main stress axis, four solutions indicate a NE–SW to ENE–WSW extension and two solutions a sub-E–W extension (Figs. 4 and 6). However, if we look at the nodal planes of the four strike-slip solutions with a NE–SW to ENE–WSW *T*-axis, we see that the azimuth for one of the two nodal planes is close to the direction of extension found in the NLB and SLB. Indeed the two northern solutions show a N95°E plane and the two southern ones a N115°E plane. In order to work out a coherence between the SLB and NLB, we assume that these mechanisms document N95°E and N115°E right-lateral strike-slip motions (Figs. 7 and 8). This interpretation is also supported by the discovery, between these two transform faults, of a NNE–SSW spreading segment around 18°40′S by Von Stackelberg et al. (1985). The complex transitional zone corresponds in fact to a ridge–ridge–ridge triple junction (Fig. 8) as proposed by Chase (1971) and Sclater et al. (1972). However, the trends of the different tectonic elements proposed here differ from these earlier authors. This transitional zone coincides also with the northern end of the Tonga platform. South of this boundary, an event with an unexpected thrust-type solution is located just west of the arc at 21°S and is difficult to interpret. Pelletier and Louat (1989) report in this area a supplementary event with a thrust-type solution. This suggests that compression immediately west of Tongatapu island could be a special feature of the Lau basin tectonics. We note also a spatial coincidence with the six thrust-type solutions east of the trench (Figs. 4 and 7).

The Fiji–North Tonga transform fault zone

We have shown that the FNTFZ is composed of two segments separated by the northern end of the Peggy ridge. The N95°E eastern segment marks the boundary between the Pacific plate and Tonga–Kermadec–North Lau plates. Along this segment, focal mechanism solutions and seismicity distribution suggest a broad zone acting as a left-lateral strike-slip fault. As there is no difference in strike between observed slip vectors and those predicted by the model RM-2, the relative motion is a pure strike-slip parallel to the direction of extension in the NLB (see before). The N70–75°E western segment marks the boundary between the P and IA plates. Along this segment, the 20° difference in azimuth between observed and RM-2 slip vectors suggests that, in addition to a left-lateral strike-slip motion, a NW–SE extensional motion must exist. The vector diagram indicates a strike-slip motion of 7 cm/y along a N75°E fault and an extensional motion of 3.5 cm/y in the N130–135°E direction (Fig. 8). This model requires a ridge–transform–transform triple junction at 178°30′W, 15°45′S between the Peggy ridge and the eastern and western segments of the FNTFZ.

Conclusions

(1) Two domains exist in the Tonga–Kermadec arc and back-arc region north and south of 19°S: a northern domain (NLB) where a sub-E–W opening occurs, and a southern domain (including SHT, NHT and SLB) where a NW–SE to ESE–WNW trending extension is present.

(2) Each basin of the southern domain has their own direction and speed of extension, which are respectively N135°E, 0.8 cm/y; N122°E, 2.1 cm/y and N111°E, 8 cm/y at 33°S (SHT), 28°S (NHT) and 24°S (SLB).

(3) Crustal consumption rate along the Tonga–Kermadec trench is respectively 7.2 cm/y, 9.6 cm/y and 16.4 cm/y in azimuth N280°E, N282°E and N284°E at 33°, 28° and 24°S.

(4) For the NLB, parallelism between slip vectors at the trench and direction of back-arc opening does not allow any accurate velocity to be calculated. However, using a 8 cm/y back-arc spreading rate deduced from magnetic anomalies and our results at 24°S, an estimate of the consumption rate is proposed at 20°S (17.1 cm/y) and at 17°S (17.8 cm/y).

(5) Contrary to the Lau basin where seismicity occurs in the center of the basin, seismicity is confined to the eastern edge of the troughs in the Havre basins. This could suggest that active spreading does not yet occur along these troughs.

(6) The back-arc spreading rate and consequently the velocity of motion TK–P increase suddenly between NHT and SLB. This 25–26°S limit coincides with the Louisville ridge–trench intersection and the 200 km long gap of seismicity along the arc.

(7) Along SHT, NHT and SLB, events having normal fault solutions occur along the eastern edges of the troughs while events showing strike-slip solutions predominate at saddles between the troughs.

(8) The N111°E extension in the SLB is compatible with the strike of the Valu Fa ridge.

(9) The N93°E trending opening tectonics in the NLB occurs along two extensional tectonic features: the N135°E Peggy ridge along which the E–W motion is decomposed into a NW–SE right-lateral strike-slip (55%) and a NE–SW extension (45%); an inferred N5°–10°E spreading center east of the Peggy ridge. Between these two features lies the North Lau microplate.

(10) The 19°S complex transitional zone between the SLB and NLB is interpreted as a ridge–ridge–ridge triple junction. This complex junction is accompanied with N95° to 115°E right-lateral transform faults.

(11) The FNTFZ comprises two domains: a N95°E trending eastern segment characterized by left-lateral strike-slip motion, and a N75°E western segment along which left-lateral strike-slip motion (7 cm/y) and N135°E extensional motion (3.5 cm/y) occur.

(12) A ridge–fracture–fracture triple junction is inferred at 178°30′W, 15°45′S between the Peggy ridge and the two segments of the FNTFZ.

(13) Tearing of the Pacific plate in the northernmost Tonga trench is immediately preceded by

an increasing N–S stretching accommodated by N–S left-lateral strike-slip motion.

(14) The present-day direction of extension of the Lau basin proposed here cannot be applied to describe all the tectonic development of the Lau basin.

Acknowledgements

We are grateful to J. Butscher for drafting the figures and to C. Baldassari for assistance in preparation of the data files. We also thank J. Dupont, J. Daniel and two anonymous reviewers for their critical reading of the manuscript.

References

Billington, S., 1980. The morphology and tectonics of the subducted lithosphere in the Tonga–Kermadec–Fiji region from seismicity and focal mechanism solutions. Ph.D. Thesis, Cornell University, Ithaca N.Y.

Chase, C.G., 1971. Tectonic history of the Fiji Plateau. Geol. Soc. Am. Bull., 82: 3087–3110.

Chen, T. and Forsyth, D.W., 1978. A detailed study of two earthquakes seaward of the Tonga-Trench: implications of mechanical behaviour of the oceanic lithosphere. J. Geophys. Res., 83: 4995–5003.

Cherkis, N.Z., 1980. Aeromagnetic investigations and sea floor spreading history in the Lau Basin and northern Fiji Plateau. UN ESCAP, CCOP/SOPAC Tech. Bull., 3: 37–45.

Dziewonski, A.M. and Woodhouse, J.H., 1983. An experiment in systematic of global seismicity: centroid-moment tensor solutions for 201 moderate and large earthquakes of 1981. J. Geophys. Res., 88 (B4): 3247–3271.

Dziewonski, A.M., Friedman, A, Giardini, D. and Woodhouse, J.H., 1983a. Global seismicity of 1982: centroid moment tensor solutions for 308 earthquakes. Phys. Earth Planet. Inter., 33: 76–90.

Dziewonski, A.M., Friedman, A. and Woodhouse, J.H., 1983b. Centroid-moment tensor solutions for January–March 1983. Phys. Earth Planet. Inter., 33: 71–75.

Dziewonski, A.M., Franzen, J.E. and Woodhouse, J.H., 1983c. Centroid-moment tensor solutions for April–June 1983. Phys. Earth Planet. Inter., 33: 243–249.

Dziewonski, A.M., Franzen, J.E. and Woodhouse, J.H., 1984a. Centroid-moment tensor solutions for July–September, 1983. Phys. Earth Planet. Inter., 34: 1–8.

Dziewonski, A.M., Franzen, J.E. and Woodhouse, J.H., 1984b. Centroid-moment tensor solutions for October–December, 1983. Phys. Earth Planet. Inter., 34: 129–136.

Dziewonski, A.M., Franzen, J.E. and Woodhouse, J.H., 1984c. Centroid-moment tensor solutions for January–March 1984. Phys. Earth Planet. Inter., 34: 209–219.

Eguchi, T., 1984. Seismotectonics of the Fiji Plateau and Lau Basin. Tectonophysics, 102: 17–32.

Everingham, I.B., 1983. Focal mechanisms for 1982 earthquakes in Fiji. Mineral Resource Dep., Suva, Fiji, Note bp 33/4.

Foucher, J.P. and shipboard scientific party of SEAPSO cruise, leg 4, 1986. Rapport scientifique de la Campagne SEAPSO leg 4: 112 pp.

Foucher, J.P., Dupont, J., Bouysse, P., Charlou, J.L., Davagnier, M., Eissen, J.P., Fouquet, Y., Gueneley, S., Harmegnies, F., Lafoy, Y., Lapouille, A., Maze, J.P., Morton, J., Ondreas, H., Ruellan, E. and Sibuet J.C., 1988. La ride de Valu Fa dans le basin de Lau méridional (sud-ouest Pacifique). C.R. Acad. Sci. Paris, 307, II: 609–616.

Giardini, D., 1984. Systematic analysis of deep seismicity: 200 centroid-moment tensor solutions between 1977 and 1980. Geophys. J.R. Astron. Soc., 77: 883–914.

Giardini, D., Dziewonski, A.M. and Woodhouse, J.H., 1985. Centroid-moment tensor solutions for 114 large earthquakes in 1977–1980. Phys. Earth Planet. Inter., 40: 259–272.

Gill, J.B., 1976. Composition and age of Lau Ridge and Basin volcanic rocks: implications for evolution of inter-arc basins. Geol. Soc. Am. Bull., 87: 1384–1395.

Hawkins, J.W., 1974. Geology of the Lau basin, a marginal sea behind the Tonga arc. In: C. Burke and C.L. Drake (Editors), Geology of Continental Margins. Springer, Berlin, pp. 505–518.

Isacks, B.L., Sykes, R. and Oliver, J., 1969. Focal mechanisms of deep and shallow earthquakes in the Tonga–Kermadec region and the tectonics of island arcs. Geol. Soc. Am. Bull., 80: 1443–1470.

Johnson, T. and Molnar, P., 1972. Focal mechanisms and plate tectonics of the Southwest Pacific. J. Geophys. Res., 77: 5000–5032.

Karig, D.E., 1970. Ridges and basins of the Tonga–Kermadec island-arc system. J. Geophys. Res., 75: 239–254.

Kelleher, J. and McCann W., 1976. Buoyant zones, great earthquakes and unstable boundaries of subduction. J. Geophys. Res., 81: 4885–4896.

Kroenke, L.W., Jouannic, C. and Woodward P., 1983. Bathymetry of the Southwest Pacific., 2nd sheet. UN ESCAP, CCOP/SOPAC.

Larue, B.M., Pontoise, B., Malahoff, A., Lapouille A. and Latham G.V., 1982. Bassins marginaux actifs du sud-ouest Pacifique: Plateau Nord-Fidjien, Bassin de Lau. Trav. Doc. ORSTOM, 147: 363–406.

Lawver, L.A., Hawkins, J.W. and Sclater, J.G., 1976. Magnetic anomalies and crustal dilation in the Lau Basin. Earth Planet. Sci. Lett., 133: 27–35.

Louat, R. and Dupont, J., 1982. Sismicité de l'arc des Tonga–Kermadec, Trav. Doc. ORSTOM, 147: 299–317.

Malahoff, A., Feden, R.H. and Fleming, H.F., 1982. Magnetic anomalies and tectonic fabric of marginal basins north of New Zealand. J. Geophys. Res., 87: 4109–4125.

Minster, J.B. and Jordan, T.H., 1978. Present day plate motions. J. Geophys. Res., 83: 5331–5354.

Morton, J. and Sleep, N.H., 1985. Seismic reflexion from a Lau basin magma chamber. In: D.W. Scholl and T.L. Vallier (Compilers and Editors), Geology and Offshore Resources of Pacific Island Arcs—Tonga region. Circum-Pac. Counc. Energy Miner. Resour., Earth Sci. Ser., 2: 441–453.

Pelletier, B., 1989. Tectonic erosion and consequent retreats of the trench and active volcanic arc due to the Lousville ridge subduction in the Tonga–Kermadec trench. Abstr. 28th Int. Geol. Congr., Washington, D.C., 1989.

Pelletier, B. and Louat, R., 1989. Mouvements relatifs des plaques dans le Sud-Ouest Pacifique. C.R. Acad. Sci. Paris., 308, II: 123–130.

Ruellan, E., Lafay, Y., Auzende, J.M., Foucher, J.P., Fouquet, Y. and Dupont, J., 1989. Oblique spreading in the northern part of the Lau back-arc basin. Geology, submitted.

Sclater, J.G., Hawkins, J.W., Mammerickx, J. and Chase, C.G., 1972. Crustal extension between the Tonga and Lau ridges: petrologic and geophysical evidence. Geol. Soc. Am. Bull., 83: 505–518.

Sykes, L.R., 1966. The seismicity and deep structure of island arcs. J. Geophys. Res., 71: 2981–3006.

Sykes, L.R., Isacks, B. and Oliver, J., 1969. Spatial distribution of deep and shallow earthquakes of small magnitude in the Fiji–Tonga region. Bull. Seismol. Soc. Am., 59: 1093–1113.

Von Stakelberg, U. and the Shipboard Scientific Party of Sonne Cruise SO-35, 1985. Hydrothermal sulfide deposit in back-arc spreading centers in the Southwest Pacific. Bundesaust. Geowiss. Rohstoffe, Circular, 2: 14 pp.

Weissel, J.K., 1977. Evolution of the Lau Basin by the growth of small plates. In: M. Talwani and W.C. Pitman (Editors), Island Arcs, Deep Sea Trenches, and Back-Arc Basins. Maurice Ewing Ser., Vol. 1 Am. Geophys. Union, Washington, D.C., pp. 429–436.